

The Energetics of Shooting Ions into the Dodecahedrane Cage

Mark Mascal

Department of Chemistry and Biochemistry, University of California, Los Angeles, California 90095

mascal@chem.ucla.edu

Received July 22, 2002

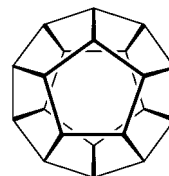
The activation barriers and energy profiles along the inclusion coordinate for the penetration of H^+ , He, Li^+ , Be^+ , Be^{2+} , and Mg^{2+} into dodecahedrane **1** vary considerably with the nature of the projectile. Using Hartree–Fock and MP2 derived structures and energies, the overall process of creating endohedral $\text{X}^{n+}@\mathbf{1}$ complexes is examined in detail.

Introduction

The concept of total incarceration of atoms, ions, or molecules within a molecular container has been a subject of enduring fascination to physical scientists.¹

In this sense, in a pre-fullerene world, the advent of dodecahedrane **1** must have been accompanied by the first awakening to the notion of complete and irreversible enclosure of one species within another. Indeed, once it became obvious that this giant of total synthesis would fall, a number of theoretical papers addressing potential guest inclusion in the $\text{C}_{20}\text{H}_{20}$ cage appeared.^{2–4} Using semiempirical and early ab initio methods, complexes between **1** and H, H^+ , H^- , H_2 , He, Li^- , Li^+ , Be, Be^+ , Be^{2+} , Na^+ , and Mg^{2+} at the geometric center of the cavity were evaluated by single-point energy calculations. Although a range of conclusions regarding the nature of these complexes was reached, there was general agreement that the interior of this molecular platonic body would at least host the H^+ and Be^{2+} ions, and the issue was shelved for 20 years until the present flurry of activity in the area of endohedral fullerene complexes led to a reconsideration of the host properties of **1**. This took form in the recent report of Cross, Saunders, and Prinzbach on the remarkable preparation of $\text{He}@\text{C}_{20}\text{H}_{20}$ by bombardment of **1** with He^+ ions,⁵ dispelling any prior notions that the cage might not be suitable for inclusion. In its wake, a theoretical investigation directly related to this work involving $\text{He}@\text{C}_{20}\text{H}_{20}$ and the hypothetical $\text{Ne}@\text{C}_{20}\text{H}_{20}$ complex was published by Jiménez-Vázquez and co-workers,⁶ who estimated a binding energy of +33.8 kcal mol⁻¹ for the former at the MP2/6-311G(d,p) level of theory. Expression of the equilibrium conditions in terms of partial pressure led to an apparent 4×10^{26} atm He within the cage. The experimental observation was a 0.01% incorporation of He in **1**. Finally, Schleyer and co-workers followed up with a detailed analysis of dodeca-

hedrane endohedrals which applied density functional theory to the problem.⁷



1

The dodecahedrane shell may be better able than the fullerenes to survive the sort of conditions which would allow species to penetrate its carbon ring network, and although its accessibility is much inferior to that of the C_{60} , improved synthetic routes now make **1** available on the gram scale in a matter of weeks.⁸ From a purely theoretical standpoint, the more favorable the binding energy, the higher the level of incorporation, the practical assumption being that conditions approaching equilibrium can be established. Although this is in principle relevant to the inclusion of neutral gas molecules in **1**, the complexation of these species is predicted to be energetically unfavorable in any case.⁶ Under more kinetic conditions, such as the bombardment of **1** by an ion beam, complexation energy itself may not be a useful indicator of the feasibility of producing a complex, since the energy required to pass through the dodecahedrane cage may dwarf the binding terms.

Previous work by Schulman and Disch had come to the intriguing conclusion that the facial complex between H^+ and **1** was actually lower in energy than the inclusion complex, whereas for Li^+ the opposite was the case.³ However, the energies were simply derived by placing the ions at the center of one of the C_5 rings and doing single point calculations with the STO-3G basis set. We now present a study in which the energetics of the passage of a range of species through the $\text{C}_{20}\text{H}_{20}$ frame is considered in detail by undertaking a potential energy

(1) Cram, D. J.; Cram, J. M. *Container Molecules and Their Guests*; Royal Society of Chemistry: Cambridge, UK, 1994.

(2) Schulman, J. M.; Disch, R. L. *J. Am. Chem. Soc.* **1978**, *100*, 5677.

(3) Disch, R. L.; Schulman, J. M. *J. Am. Chem. Soc.* **1981**, *103*, 3297.

(4) Dixon, D. A.; Deerfield, D.; Graham, G. D. *Chem. Phys. Lett.* **1981**, *78*, 161.

(5) Cross, R. J.; Saunders, M.; Prinzbach, H. *Org. Lett.* **1999**, *1*, 1479.

(6) Jiménez-Vázquez, H. A.; Tamariz, J.; Cross, R. J. *J. Phys. Chem. A* **2001**, *105*, 1315.

(7) Moran, D.; Stahl, F.; Jemmis, E. D.; Schaefer, H. F., III; Schleyer, P. v. R. *J. Phys. Chem. A* **2002**, *106*, 5144.

(8) Bertau, M.; Wahl, F.; Weiler, A.; Scheumann, K.; Worth, J.; Keller, M.; Prinzbach, H. *Tetrahedron* **1997**, *53*, 10029.

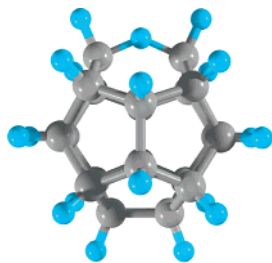


FIGURE 1. Modeled representation of the $1H^+$ exohedral complex at MP2/6-311G(d,p).

TABLE 1. HF/6-311g(d,p) and MP2/6-311g(d,p) Endohedral Complexation Energies (kcal mol⁻¹)^a

species	E_{HF}	E_{MP2}	symmetry
$H^+@1^b$	-42.89	-63.63	I_h
$He@1$	41.67	34.22	I_h
$Li^+@1$	0.85	-6.90	I_h
$Be^+@1$	41.20	1.35	C_{5v}
$Be^{2+}@1$	-201.38	-223.69	C_{5v}
$Mg^{2+}@1$	-88.69	-101.99	I_h

^a Values include BSSE correction and HF/6-311G(d,p) zero-point energy. ^b Stationary point with three imaginary frequencies.

surface scan including geometry optimizations to derive energy minimum values at each point.

Computational Methods

On the basis of previous reports,^{2-4,6,7} it appeared most reasonable to model the interaction between **1** and H^+ , He , Li^+ , Be^+ , Be^{2+} , and Mg^{2+} . We first determined the endohedral binding energies at the MP2 level of theory, also used by Jiménez-Vázquez and co-workers in their study,⁶ which is generally considered highly appropriate for the study of subtle noncovalent interactions.

Each calculation started with an HF/6-31G(d) geometry optimization and frequency calculation starting from C_1 symmetry with orbital symmetry disabled during the SCF procedure to allow all degrees of freedom to be sampled. Default convergence criteria in Gaussian98 were used.⁹ The resulting structures were then symmetrized to their highest point group, and the HF/6-31G(d) optimization and frequency calculations repeated in order to ensure the assumption of symmetry was valid for these systems, i.e., that no significant changes in structure, energy, or vibrational frequencies were introduced. The minimized, symmetrical structures were then reoptimized at HF/6-311G(d,p) and MP2/6-311G(d,p). Frequencies were calculated and stationary points characterized with the HF method, but this was not practical at MP2, and (unscaled) HF/6-311G(d,p) zero-point energy corrections were applied in this case. Basis set superposition energy (BSSE) corrections were done using the Boys–Bernardi counterpoise method.¹⁰

A relaxed HF/6-31G(d) potential energy surface scan was then performed for each species at selected points along an axis defined by the symmetry center of **1** and the center of one cyclopentane ring of the cage. Geometry optimizations were performed at each point while constraining the distances along the axis and/or symmetry of the system (either I_h or C_{5v} , as appropriate). Natural endo- and exohedral complex minima energy values were derived by performing optimizations in the absence of distance constraints and confirming the minima by frequency analysis.

Results and Discussion

Efforts focused first on $H^+@C_{20}H_{20}$, since the consensus in earlier studies was that this complex would be stable relative to the components at infinite separation, with endohedral binding energies estimated at -19.1 (PRDDO),⁴ -42.4 (STO-3G),³ and -130 (INDO)² kcal mol⁻¹. In the previous work, only energies were calculated and no minimization or characterization of the PE surface through vibrational analysis was carried out. Our cal-

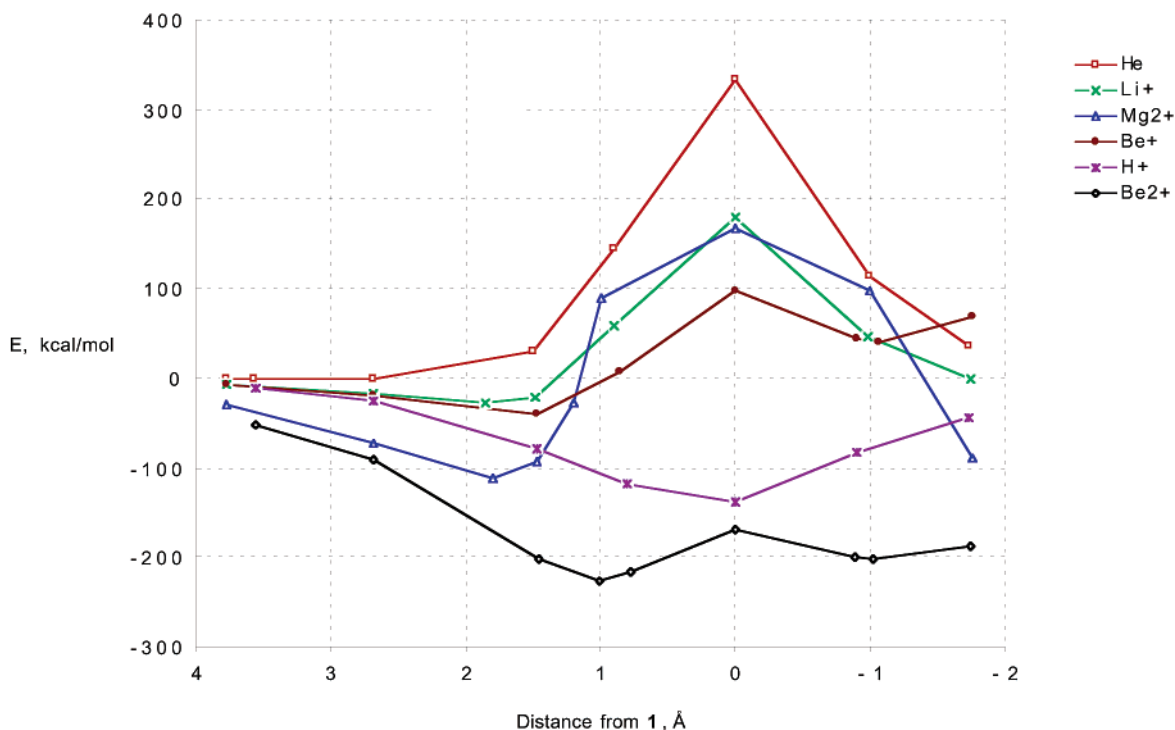


FIGURE 2. Graphical representation of the HF/6-31G(d) potential energy profiles of the approach of H^+ , He , Li^+ , Be^+ , Be^{2+} , and Mg^{2+} toward the symmetry center of **1** along a C_{5v} symmetry axis. The 0 Å point represents the center of the cyclopentane ring through which the inclusion coordinate passes.

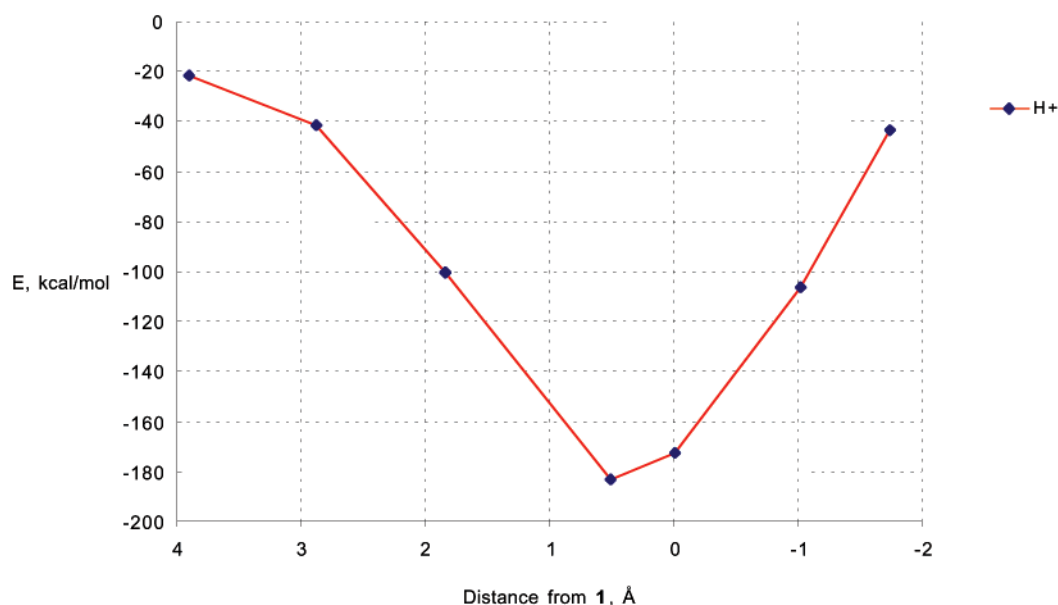


FIGURE 3. Graphical representation of the HF/6-31G(d) potential energy profile of the approach of H^+ toward the symmetry center of **1** along a C_{2v} symmetry axis. The 0 Å point represents the center of a C–C bond through which the inclusion coordinate passes.

culations confirm that, as predicted, H^+ is stabilized in the center of the $\text{C}_{20}\text{H}_{20}$ sphere (Table 1), but that the imposition of I_h symmetry produces three imaginary Hessian frequencies. The animation of these frequencies shows a displacement of the proton toward C–C bonds bisecting all three principal axes. Indeed, the removal of symmetry constraints results in a minimum where H^+ has escaped the dodecahedrane shell and inserted into a C–C bond to give an exohedral 3-center-2-electron complex **1H**⁺ (Figure 1) which is 172.8 kcal mol^{−1} lower in energy than **1**.

This indicates that, contrary to the earlier reports, no endohedral complex between H^+ and **1** is possible. Although the above suggests that small, positively charged species can be effectively “solvated” by **1**, the bare proton is too reactive to be contained. Its potential energy profile (Figure 2) is unique in that it actually experiences a minimum in energy when passing through the C_5 ring.

(9) Frisch, M. J.; Trucks, G. W.; Schlegel, H. B.; Scuseria, G. E.; Robb, M. A.; Cheeseman, J. R.; Zakrzewski, V. G.; Montgomery, J. A., Jr.; Stratmann, R. E.; Burant, J. C.; Dapprich, S.; Millam, J. M.; Daniels, A. D.; Kudin, K. N.; Strain, M. C.; Farkas, O.; Tomasi, J.; Barone, V.; Cossi, M.; Cammi, R.; Mennucci, B.; Pomelli, C.; Adamo, C.; Clifford, S.; Ochterski, J.; Petersson, G. A.; Ayala, P. Y.; Cui, Q.; Morokuma, K.; Salvador, P.; Dannenberg, J. J.; Malick, D. K.; Rabuck, A. D.; Raghavachari, K.; Foresman, J. B.; Cioslowski, J.; Ortiz, J. V.; Baboul, A. G.; Stefanov, B. B.; Liu, G.; Liashenko, A.; Piskorz, P.; Komaromi, I.; Gomperts, R.; Martin, R. L.; Fox, D. J.; Keith, T.; Al-Laham, M. A.; Peng, C. Y.; Nanayakkara, A.; Challacombe, M.; Gill, P. M. W.; Johnson, B.; Chen, W.; Wong, M. W.; Andres, J. L.; Gonzalez, C.; Head-Gordon, M.; Replogle, E. S.; Pople, J. A. *Gaussian 98*, Revision A.11; Gaussian, Inc.: Pittsburgh, PA, 2001.

(10) Boys, S. F.; Bernardi, F. *Mol. Phys.* **1970**, *19*, 553.

(11) Four of the species studied have calculated electron affinities greater than that of the dodecahedrane radical cation (185.5 kcal mol^{−1}), i.e., H^+ (312.6 kcal mol^{−1}), He^+ (540.6 kcal mol^{−1}), Be^{2+} (417.7 kcal mol^{−1}), and Mg^{2+} (339.3 kcal mol^{−1}). However, in all cases except He^+ , the natural exo- and endohedral complexes show no $\text{rhf} \rightarrow \text{uhf}$ instabilities. As the ions are moved away from **1**, at some point (between 2 and 3 Å for H^+ and Be^{2+} , and between 3 and 4 Å for Mg^{2+}) the singlet diradical state becomes energetically favored over the closed-shell description. This suggests that some electron-transfer processes may be involved in the approach of these ions to **1**, the energetic contributions to which, however, are not known.

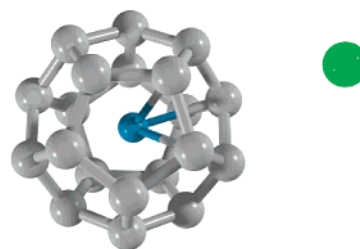


FIGURE 4. Modeled representation of the $\text{Li}^+@C_{20}\text{H}_{20} \text{Cl}^-$ ion pair at HF/6-31+G(d). Hydrogens are omitted for clarity.

Unconstrained minimization with the proton external to **1** does not, however, lead to the facial complex, but to hydride abstraction to give the dodecahedrane carbocation and H_2 , the combination of which lies 167.7 kcal mol^{−1} below **1** or 5.1 kcal mol^{−1} above the complex in Figure 1. Minimization along an alternative trajectory from the symmetry center of **1** through the midpoint of a C–C bond (which includes the complex in Figure 1) gives the curve shown in Figure 3.

Since $\text{He}@C_{20}\text{H}_{20}$ is produced by either exposing **1** to an He^+ ion beam or by fast atom bombardment with He ,⁵ we sought to determine the energy for the ingress and escape of both He^+ and He . While this presented no problems for neutral He , which shows the classic repulsive nature of two neutral, closed shell species (Figure 2), the He^+ cation simply removes an electron from **1**, accompanied by a 355 kcal mol^{−1} exotherm, and no realistic modeling of the approach of He^+ to **1** is possible.¹¹

After helium, perhaps the next most obvious candidate for inclusion would be the lithium cation. Not only is endohedral complexation of Li^+ energetically favorable at MP2 but, unlike H^+ , the stationary point is confirmed as a minimum by frequency analysis. The enthalpy of inclusion is about a factor of 10 lower than that of the proton, one reason for which appears to be the strain of

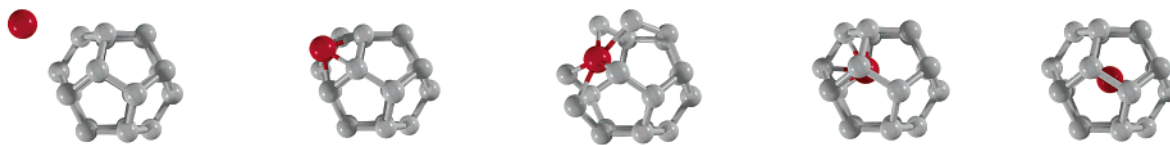


FIGURE 5. Modeled representation of the penetration of **1** by Mg^{2+} , using geometries calculated at HF/6-31G(d). Hydrogens are omitted for clarity.

TABLE 2. Key Energies (kcal mol⁻¹) on the Inclusion Coordinate in Figure 2, Activation Barriers (E_a), and C–C Bond Distortion during Entry into **1**

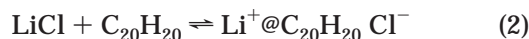
interaction	E_{exo}	E_{facial}^a	E_{endo}	E_a	C–C ^b
1 + H^+		–138.0	–42.9		1.63
1 + He	–0.04	333.8	37.4	333.9	1.85
1 + Li^+	–26.3	180.3	–1.2	206.7	1.87
1 + Be^+	–40.3	98.4	40.7	138.7	1.83
1 + Be^{2+}	–226.4	–168.6	–201.8	57.8	1.85
1 + Mg^{2+}	–110.6	168.5	–88.7	279.1	2.23

^a All facial complexes are stationary points with one or more imaginary vibrational frequencies. ^b The optimized C–C distance in **1** is 1.55 Å.

hosting the larger ion. The cage distorts by elongating all 30 C–C bonds about 1% on complexation of Li^+ , compared to only about 0.5% for H^+ . The energetics of inclusion suggest a favorable equilibrium for eq 1. Internal partition functions largely cancel out due to the



overall small changes in vibrational modes of the system on complexation, so an equilibrium constant of about 4 M⁻¹ can be derived from the MP2 energy value and the mass-derived thermal wavelengths, compared to 6×10^{-30} M⁻¹ for $\text{He}@\text{C}_{20}\text{H}_{20}$. The energetics of cage penetration, however, reveal a potential energy curve not very different from that of helium, with about 200 kcal mol⁻¹ required to pass through the C_5 face and attendant splaying out of the C–C bonds to 1.87 Å during entry (Table 2). Including a counterion in the equation leads to the equilibrium expression eq 2. Using the HF method and the 6-31+G(d) basis set including diffuse functions to more accurately model the orbitals of the anion, an enthalpy of +79.8 kcal mol⁻¹ is derived for the production of $\text{Li}^+@\text{C}_{20}\text{H}_{20} \text{Cl}^-$ from gaseous LiCl and **1**.



Interestingly, the symmetry of the $\text{Li}^+@\text{C}_{20}\text{H}_{20}$ complex changes in the presence of a counterion to C_{5v} , with the cation displaced from the center of the sphere toward the face occupied by the anion (Figure 4). The equilibrium concentration of the complex ion pair would of course in these circumstances be vanishingly small, again emphasizing that the binding energies tell us only whether the species can exist, not whether it can be made.

The work of Schleyer et al. had concluded that the monovalent Be^+ complex formed a C_{5v} symmetric endohedral complex with **1** stable by –1.3 kcal mol⁻¹ relative to the isolated components.⁷ We have also located this minimum at MP2; however, we find complexation endothermic by +1.4 kcal mol⁻¹. Be^+ also gives the least stable I_h complex of all those considered in this study, which is not a minimum but characterized by three

imaginary vibrational frequencies. Figure 2 shows that as Be^+ approaches **1** the energy decreases until an inflection point at the exohedral C_{5v} complex is reached, after which it climbs in the direction of the facial complex. The energy then again dips toward the endohedral C_{5v} minimum before making its final ascent to the dodecahedrane core. An analogous potential energy profile is observed for the Be^{2+} ion, which, however, interacts much more strongly with **1** such that every point of the curve is well below the abscissa.

Finally, the third-row Mg^{2+} ion also interacts exothermically with **1**, forming first a stable C_{5v} exohedral complex. The energy then increases to 168 kcal mol⁻¹ in the C_5 plane, which appears modest considering the gap it opens in the cage, with distances of 2.23 Å between the carbons surrounding the metal (Table 2). The endohedral complex has I_h symmetry and is the most stable such complex after that of Be^{2+} . The insertion of Mg^{2+} into **1** is depicted graphically in Figure 5.

Conclusions

Energies for the endohedral complex formation between **1** and Li^+ , Be^+ , Be^{2+} , and Mg^{2+} have been calculated for the first time at the MP2 level of theory. The values fall between those calculated with the HF method and those previously calculated using density functional theory.⁷ Working in the gas phase, the data in Table 2 approximate the relative, minimum energetic barriers to penetration of the dodecahedrane surface by He and the Li^+ , Be^+ , Be^{2+} , and Mg^{2+} ions. Since all of these species interact more strongly with the exterior of than the interior of **1**, the cost of dissociating the exo complex is taken into account in deriving activation energies. Only H^+ can pass through the cage without energetic penalty, although the nature of the stable exo complex indicates that no endo complexation is possible. The energetic requirements for introducing Be^{2+} into **1** are modest, while those for Be^+ , Li^+ , and Mg^{2+} are considerably higher. The results suggest that ion beam energies which are lower relative to the measured 100 eV threshold⁵ for the introduction of He into **1** may apply to the ions presented in this study.

Acknowledgment. The author is indebted to Prof. Kendall N. Houk and Dr. Andrew Leach for helpful advice. This work was supported in part by the National Computational Science Alliance under grant CHE02-0003N and utilized the University of Kentucky HP Superdome complex.

Supporting Information Available: Cartesian coordinates of the endohedral, exohedral, and facial complexes described in this work at the highest level of theory studied. This material is available free of charge via the Internet at <http://pubs.acs.org>.

JO026226X